IEEE Access
Multidisciplinary ⋮ Rapid Review ⋮ Open Access Journal

Received March 25, 2020, accepted April 5, 2020, date of publication April 20, 2020, date of current version May 11, 2020.

Digital Object Identifier 10.1109/ACCESS.2020.2988891

On Inadequacy of Sequential Design of Experiments for Performance-Driven Surrogate Modeling of Antenna Input Characteristics

ANNA PIETRENKO-DABROWSKA[1], (Senior Member, IEEE), AND SLAWOMIR KOZIEL[1,2], (Senior Member, IEEE)

[1]Faculty of Electronics, Telecommunications and Informatics, Gdansk University of Technology, 80-233 Gdansk, Poland
[2]Engineering Optimization and Modeling Center, Reykjavik University, 101 Reykjavik, Iceland

Corresponding author: Anna Pietrenko-Dabrowska (anna.dabrowska@pg.edu.pl)

This work was supported in part by the Icelandic Centre for Research (RANNIS) under Grant 174114051 and Grant174573051, and in part by the National Science Centre of Poland under Grant 2018/31/B/ST7/02369.

ABSTRACT Design of contemporary antennas necessarily involves electromagnetic (EM) simulation tools. Their employment is imperative to ensure evaluation reliability but also to carry out the design process itself, especially, the adjustment of antenna dimensions. For the latter, traditionally used parameter sweeping is more and more often replaced by rigorous numerical optimization, which entails considerable computational expenses, sometimes prohibitive. A potentially attractive way of expediting the simulation-based design procedures is the replacement of expensive EM analysis by fast surrogate models (or metamodels). Unfortunately, due to the curse of dimensionality and considerable nonlinearity of antenna characteristics, applicability of conventional modeling methods is limited to structures described by small numbers of parameters within narrow ranges thereof. A recently proposed nested kriging technique works around these issues by allocating the surrogate model domain within the regions containing designs that are of high quality with respect to the selected performance figures. This paper investigates whether sequential design of experiments (DoE) is capable of enhancing the modeling accuracy over one-shot space-filling data sampling originally implemented in the nested kriging framework. Numerical verification carried out for two microstrip antennas indicates that no noticeable benefits can be achieved, which contradicts the commonsense expectations. This result can be explained by a particular geometry of the confined domain of the performance-driven surrogate. As this set consists of nearly-optimum designs, the average nonlinearity of the antenna responses therein is almost location independent, therefore optimum training data allocation should be close to uniform. This is indeed corroborated by our experiments.

INDEX TERMS Antenna design, surrogate modeling, approximation models, kriging interpolation, performance-driven modeling, sequential sampling.

I. INTRODUCTION

The design of modern antennas is a demanding and multi-stage endeavour that involves conceptual development, topology evolution, as well as the adjustment of geometry parameters [1]–[3]. The latter may be quite extensive and often pertains to all antenna dimensions [4]. The reasons are strictly related to geometrical complexity of contemporary antenna systems where the fulfillment of stringent performance requirements [5] and implementation of various functionalities, e.g., circular polarization [6], multi-band [7] or MIMO operation [8], pattern/polarization diversity [9], let alone meeting additional requirements such as reduction of the physical size of the radiator [10], [11], calls for unconventional layouts [12]–[19]. These include incorporation of stubs [12], [13], slots [14], [15], defected ground structures [16], [17] or complex (e.g., spline-parameterized) profiles [18], [19] the exact effects of which cannot be quantified using analytical or equivalent network representations. Thus, utilization of full-wave electromagnetic (EM) simulation tools is imperative at all design stages to ensure the reliability of antenna evaluation [20], [21]. It is especially

The associate editor coordinating the review of this manuscript and approving it for publication was Giambattista Gruosso.

crucial in parameter tuning, which is nowadays frequently realized through rigorous numerical optimization. The high computational cost of such procedures—a result of massive EM analyses required by both local [22] and global [23] search routines, is a serious practical problem. It is even more pronounced for uncertainty quantification procedures, especially robust (tolerance-aware) design [24], [25].

Expediting simulation-driven design is a practical necessity. It can be accomplished using strictly algorithmic means, the example of which is the incorporation of adjoint sensitivities [26] into gradient optimization [27], [28]. Non-intrusive methods include gradient-based routines with sparse sensitivity updates, e.g., [29], [30]. Computational speedup can also be obtained using variable-fidelity simulation models such as equivalent networks in the case of microwave components [31] or coarse-mesh EM analysis in the design of antenna structures [32]. In either case, the low-fidelity model has to undergo an appropriate enhancement to be used as a reliable predictor. Popular techniques include space mapping [33] as well as various response correction schemes (manifold mapping [34], adaptive response scaling [35], shape-preserving response prediction [36]). For certain purposes, especially global optimization, machine learning techniques are often employed [37], [38], typically in connection with surrogate modeling methods [39] and adaptive sampling [40]. Local surrogates are becoming indispensable for uncertainty quantification, either to replace EM analysis when performing Monte Carlo analysis [41] or to directly yield the statistical moments of the system outputs (e.g., polynomial chaos expansion [42]).

A more aggressive approach is to replace expensive EM simulations in their entirety by globally accurate surrogates [43]. Ensuring a sufficient predictive power of the metamodel enables conducting all conceivable simulation-based design tasks at a negligible cost. The initial expenditures related to training data acquisition, even if considerable, may be justified by multiple use of the model. Due to their generality, data-driven (or approximation) surrogates are by far the most popular [44]. Some widely applied techniques include kriging [45], Gaussian process regression [46], radial basis functions [47], artificial neural networks [48], and, recently, polynomial chaos expansion [49]. Although appealing, practical realization of the above concept is hindered by several factors including high nonlinearity of antenna characteristics and the curse of dimensionality, i.e., a rapid increase of the training data set size required to render a reliable model as a function of the number of antenna parameters. Another issue are utility demands: design-ready surrogate should be valid over broad ranges of the system operating conditions, material parameters (e.g., substrate permittivity) and geometry parameters. Establishing an accurate model that fulfills such conditions is challenging for modern multi-parameter antennas to the extent of being virtually impossible beyond a few variables with narrow ranges thereof [44]. Available mitigation techniques, e.g., high-dimensional model representation (HDMR) [50], smart basis function selection schemes (orthogonal matching pursuit, OMP [51], least-angle regression, LAR [52]), or variable-fidelity surrogates (co-kriging [53], Bayesian model fusion [54]) are only applicable to specific situations.

A recently proposed performance-driven modeling offers an alternative approach to overcoming the dimensionality and parameter range issues [55]. As suggested in [55], by constraining the model domain to a region that contains high quality design with respect to performance figures relevant to the antenna structure at hand, it is possible to render the surrogate that is accurate and valid over wide ranges of operating conditions (e.g., antenna center frequency [56] or permittivity/thickness of the substrate antenna is implemented on [57]). At the same time, the required number of training samples is significantly lower than for conventional methods. Identification of the region of interest is carried out using a pre-optimized set of reference designs [55]. Due to a complex geometry of the constrained domain, some practical problems may arise related to design of experiments but also model optimization [58]. These have been greatly alleviated by the nested kriging framework [59], the formulation of which involves a surjective transformation between the unity interval and the model domain.

This paper investigates whether introducing sequential design of experiments (DoE) into the nested kriging framework may bring further benefits (in terms of improving the predictive power of the surrogate) over the uniform sampling originally implemented in [59]. Sequential DoEs [60], especially the exploitative ones [20] aim at identifying and filling in the regions characterized by higher nonlinearity of the system outputs. This allows for redistribution of the training data samples by putting more emphasis on such areas while sparing samples on the plateau or low-nonlinearity regions. Here, the infill criterion is maximization of the mean square error [61] because the overall goal is to improve the global accuracy of the surrogate. Numerical experiments conducted for two dual-band microstrip antennas indicates that sequential DoE does not bring any computational benefits over the uniform sampling. This is an interesting and counterintuitive result. Notwithstanding, it can be explained by the specific geometry of the domain of the nested kriging surrogate model, i.e., the fact that it only contains designs that are nearly-optimum with respect to the selected figures of interest. The latter implies that the frequency-averaged nonlinearity of the antenna responses is almost location independent. Consequently, the expected optimum allocation of the training data samples should be close to uniform. This seems to be an inherent feature of performance-driven modelling techniques in general, and the nested-kriging framework in particular.

II. SURROGATE MODELING BY NESTED KRIGING. UNIFORM AND SEQUENTIAL SAMPLING

This section briefly recalls the nested kriging modelling method with the emphasis on the uniform domain sampling technique utilized in the original version of the framework.

Subsequently, incorporation of sequential sampling into the nested kriging methodology is discussed. Section III compares the predictive power surrogate model constructed using these two sampling strategies and provides qualitative explanations for the obtained results.

A. NESTED KRIGING MODELING FORMULATION

The nested kriging procedure constructs two kriging interpolation surrogates [45]. The first-level model serves for identifying the domain for the second-level model, being the actual surrogate that represents the antenna characteristics. The surrogate domain X_S is a confined region of the box-constrained design space X, typically delimited by the lower bounds $\boldsymbol{l}$ and the upper bounds $\boldsymbol{u}$ for design variables. The domain X_S accommodates high-quality designs, i.e., the designs that are optimal or nearly-optimal w.r.t. the performance figures that are of interest in a given design context. Exemplary figures of merit may refer to antenna electrical characteristics (e.g., operating frequencies in the case of multi-band antennas) or material parameters, such as relative permittivity of dielectric substrate the antenna is to be implemented on. These are denoted as f_k, $k = 1, \ldots, N$. The ranges of the performance figures $f_{k.\min} \le f_k^{(j)} \le f_{k.\max}$, $k = 1, \ldots, N$, for which the surrogate is to be valid for, delimit the objective space F.

The first-level kriging surrogate $\boldsymbol{s}_I(\boldsymbol{f})$ is rendered using the training data set $\{\boldsymbol{f}^{(j)}, \boldsymbol{x}^{(j)}\}_{j=1,\ldots,p}$, where $\boldsymbol{x}^{(j)} = [x_1^{(j)} \ldots x_n^{(j)}]^T$ are the designs optimal w.r.t. the selected performance vectors $\boldsymbol{f}^{(j)} = [f_1^{(j)} \ldots f_N^{(j)}]$; $\boldsymbol{x}^{(j)}$ are referred to as the reference designs. Thus, the first-level model $\boldsymbol{s}_I(\boldsymbol{f})$, that maps the objective space F into the parameter space X, is an inverse model, which, for a given performance vector $\boldsymbol{f} \in F$, yields a corresponding vector $\boldsymbol{x} \in X$. The intended domain for the surrogate is to contain all the designs that are optimal w.r.t. all performance vectors $\boldsymbol{f} \in F$. As the set $\boldsymbol{s}_I(F) \subset X$ is a mere approximation of such a region, it has to be expanded. This is carried out by an orthogonal extension of $\boldsymbol{s}_I(F)$ in its normal directions. Let us denote by $\{\boldsymbol{v}_n^{(k)}(\boldsymbol{f})\}$, $k = 1, \ldots, n-N$, the orthonormal basis of vectors normal to $\boldsymbol{s}_I(F)$ at $\boldsymbol{f} \in F$ [59]. Furthermore, we denote by $\boldsymbol{x}_d = \boldsymbol{x}_{\max} - \boldsymbol{x}_{\min}$ the ranges of design variables within $\boldsymbol{s}_I(F)$), where $\boldsymbol{x}_{\max} = \max\{\boldsymbol{x}^{(k)}, k = 1, \ldots, p\}$, $\boldsymbol{x}_{\min} = \min\{\boldsymbol{x}^{(k)}, k = 1, \ldots, p\}$. Using these, the following manifolds can be defined

$$M_{\pm} = \left\{ \boldsymbol{x} \in X : \boldsymbol{x} = \boldsymbol{s}_I(\boldsymbol{f}) \pm \sum\nolimits_{k=1}^{n-N} \alpha_k(\boldsymbol{f}) \boldsymbol{v}_n^{(k)}(\boldsymbol{f}) \right\} \quad (1)$$

where

$$\begin{aligned} \boldsymbol{\alpha}(\boldsymbol{f}) &= [\alpha_1(\boldsymbol{f}) \ \ldots \ \alpha_{n-N}(\boldsymbol{f})]^T \\ &= 0.5T \left[|\boldsymbol{x}_d \boldsymbol{v}_n^{(1)}(\boldsymbol{f})| \ \ldots \ |\boldsymbol{x}_d \boldsymbol{v}_n^{(n-N)}(\boldsymbol{f})| \right]^T \end{aligned} \quad (2)$$

are the extension coefficients with T being a domain thickness parameter. The domain X_S is then established as

$$X_S = \left\{ \begin{array}{c} \boldsymbol{x} = \boldsymbol{s}_I(\boldsymbol{f}) + \sum_{k=1}^{n-N} \lambda_k \alpha_k(\boldsymbol{f}) \boldsymbol{v}_n^{(k)}(\boldsymbol{f}) : \boldsymbol{f} \in F, \\ -1 \le \lambda_k \le 1, \ k = 1, \ldots, n-N \end{array} \right\} \quad (3)$$

The second-level kriging surrogate is set up in X_S using the data pairs $\{\boldsymbol{x}_B^{(k)}, \boldsymbol{R}(\boldsymbol{x}_B^{(k)})\}_{k=1,\ldots,NB}$, with $\boldsymbol{R}$ being the response of the EM antenna model. Allocation of the training samples is of paramount importance for model reliability. Section II.B outlines the design of experiments strategy utilized by the original nested kriging framework [59], which is replaced in this work by the sequential sampling scheme as described in Section II.C.

B. DESIGN OF EXPERIMENTS FOR NESTED KRIGING: UNIFORM SAMPLING

In original nested kriging, one-shot design of experiments is carried out, i.e., the entire data set is allocated prior to constructing the model [59]. Despite a potentially complex geometry of the model domain, the space-filling sampling is greatly facilitated by exploiting the domain definition (3) and a two-stage surjective transformation from a unit hypercube $[0,1]^n$ onto X_S. In the first step, the data samples $\{\boldsymbol{z}^{(k)}\}$, $k = 1, \ldots, N_B$, $\boldsymbol{z}^{(k)} = [z_1^{(k)} \ldots z_n^{(k)}]^T$, are uniformly distributed using a Latin Hypercube Sampling [62], and mapped using an auxiliary transformation h_1 onto a Cartesian product $F \times [-1,1]^{n-N}$

$$\begin{aligned} \boldsymbol{y} = h_1(\boldsymbol{z}) = h_1([z_1 \ \ldots \ z_n]^T) = [&f_{1.\min} + z_1(f_{1.\max} - f_{1.\min}) \\ &\ldots\ldots f_{N.\min} + z_N(f_{N.\max} - f_{N.\min})] \\ &\times [-1 + 2z_{N+1} \ \ldots \ -1 + 2z_n] \end{aligned} \quad (4)$$

whereas the second transformation h_2 maps $F \times [-1,1]^{n-N}$ into X_S as

$$\begin{aligned} \boldsymbol{x} = h_2(\boldsymbol{y}) = h_2([y_1 \ \ldots \ y_n]^T) &= \boldsymbol{s}_I([y_1 \ \ldots \ y_N]^T) \\ &+ \sum_{k=1}^{n-N} y_{N+k} \alpha_k([y_1 \ \ldots \ y_N]^T) \boldsymbol{v}_n^{(k)}([y_1 \ \ldots \ y_N]^T) \end{aligned} \quad (5)$$

The samples $\boldsymbol{x}_B^{(k)}$ within the constrained domain X_S (being a subset of the design space X) are obtained by applying a composed transformation H: $[0,1]^n \to X_S$, $H(\cdot) = h_2(h_1(\cdot))$, to the data set $\{\boldsymbol{z}^{(k)}\}$ as follows

$$\boldsymbol{x}_B^{(k)} = H(\boldsymbol{z}^{(k)}) = h_2(h_1(\boldsymbol{z}^{(k)})) \quad (6)$$

Note that the uniform distribution of $\{\boldsymbol{z}^{(k)}\}$ is understood with respect to the objective space F. This is generally more advantageous over a uniform distribution in X_S because of a normally nonlinear dependence between the performance figures and the geometry parameter values corresponding to the designs optimized with respect to these figures. Figure 1 shows a graphical illustration of the sampling procedure outlined above.

C. SEQUENTIAL DESIGN OF EXPERIMENTS FOR NESTED KRIGING

In this section, sequential design of experiments is considered as an alternative sampling strategy for the nested kriging modeling framework. The aim is to improve the predictive power of the surrogate model without increasing the training data set size. As explained in Section II.B, in original nested kriging, the samples are allocated using a one-shot procedure, based on LHS [62] and a mapping from

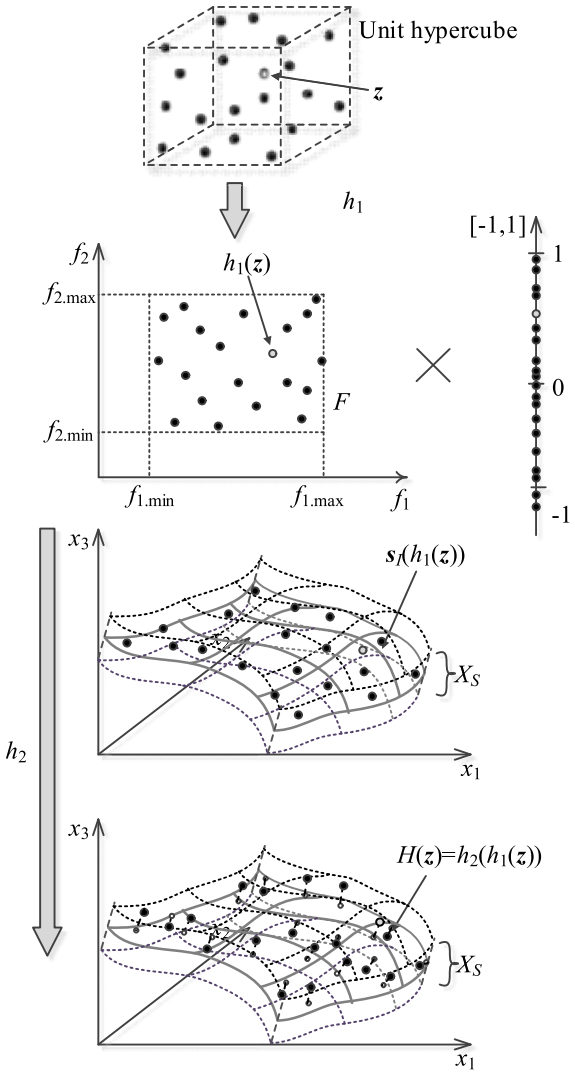

FIGURE 1. One-shot sampling procedure in the domain X_S (for two-dimensional objective space F and three-dimensional parameters space X) [59]: (i) function h_1 (see (4)) maps LHS-allocated samples onto the Cartesian product of F and $[-1, 1]_{n-N}$; (ii) next, function h_2 (see (5)) maps the samples onto X_S; penultimate picture from the bottom shows samples $s_f(h_1(z))$ mapped into the image $s_f(F)$ of F; (iii) orthogonally relocated samples within entire X_S (see (6)).

the normalized domain (unity interval) onto the surrogate domain [59]. One of the objectives of sequential sampling [60], [63] is to concentrate the training data samples in the regions of higher nonlinearity of the system outputs. This normally allows for reducing the modeling error as compared to uniform distributions, assuming comparable training data set sizes [64].

In this work, we focus on exploitation-based sequential sampling [20], where the new (infill) data samples are allocated iteratively using information acquired at the previously allocated points. To that end, the choice of kriging interpolation, among various data-driven surrogates, is beneficial, because the kriging surrogate provides information about the expected model error [65]. Here, the adopted infill criterion is maximization of the mean square error [61].

For the convenience of the reader, a brief formulation of kriging interpolation is provided below. Let $\boldsymbol{X}_{B.KR} = \{\boldsymbol{x}^1, \boldsymbol{x}^2, \ldots, \boldsymbol{x}^{NB}\}$ be the training set with $\boldsymbol{R}_f(\boldsymbol{X}_{B.KR})$ referring to the corresponding high-fidelity model outputs. The kriging surrogate $\boldsymbol{s}_{KR}(\boldsymbol{x})$ is defined as follows [45]

$$\boldsymbol{s}_{KR}(\boldsymbol{x}) = \boldsymbol{\mu}\boldsymbol{\beta} + \boldsymbol{\rho}(\boldsymbol{x}) \cdot \boldsymbol{\Psi}^{-1} \cdot (\boldsymbol{R}_f(\boldsymbol{X}_{B.KR}) - \boldsymbol{\varphi}\boldsymbol{\beta}) \tag{7}$$

In (4), $\boldsymbol{\mu}$ stands for a $N_B \times t$ model matrix of the training set $\boldsymbol{X}_{B.KR}$ and $\boldsymbol{\varphi}$ refers to a $1 \times t$ vector of the evaluation point $\boldsymbol{x}$; with t being the number of terms used in the regression function [66] described by the coefficients $\boldsymbol{\beta}$

$$\boldsymbol{\beta} = (\boldsymbol{X}_{B.KR}^T \boldsymbol{\Psi}^{-1} \boldsymbol{X}_{B.KR})^{-1} \boldsymbol{X}_{B.KR} \boldsymbol{\Psi}^{-1} \boldsymbol{R}_f(\boldsymbol{X}_{B.KR}) \tag{8}$$

whereas $\boldsymbol{\rho}(\boldsymbol{x}) = \left[\psi(\boldsymbol{x}, \boldsymbol{x}^1), \ldots, \psi(\boldsymbol{x}, \boldsymbol{x}^{N_B})\right]$ is an $1 \times N_B$ vector of correlations between $\boldsymbol{x}$ and $\boldsymbol{X}_{B.KR}$, and $\boldsymbol{\Psi} = [\Psi_{i,j}]$ is a correlation matrix with $\Psi_{i,j} = \psi(\boldsymbol{x}^i, \boldsymbol{x}^j)$. Frequently, the following correlation function is utilized [67]

$$\psi(\boldsymbol{x}, \boldsymbol{x}') = \exp\left(\sum_{k=1}^{n} -\theta_k |x^k - x'^k|^P\right) \tag{9}$$

where θ_k, $k = 1, \ldots, n$, (n being the parameter space dimensionality), are the hyperparameters, whereas P is typically constant and decides upon the prediction 'smoothness' (for many practical problems $P = 2$, i.e., Gaussian correlation function, is assumed). The Maximum Likelihood Estimate (MLE) of hyperparameters θ_k [67] is $(\theta_1, \ldots, \theta_n) = \arg\min -(N_B/2)\ln(\hat{\sigma}^2) - 0.5\ln(|\boldsymbol{\Psi}|)$, where the variance is expressed as $\hat{\sigma}^2 = (\boldsymbol{R}_f(\boldsymbol{X}_{B.KR}) - \boldsymbol{\varphi}\boldsymbol{\beta})^T \boldsymbol{\Psi}^{-1} (\boldsymbol{R}_f(\boldsymbol{X}_{B.KR}) - \boldsymbol{\varphi}\boldsymbol{\beta})/N_B$, and $|\boldsymbol{\Psi}|$ stands for the determinant of $\boldsymbol{\Psi}$. If no extrapolation is required, the regression function is assumed constant, i.e., $\boldsymbol{\varphi} = [1 \ldots 1]^T = \boldsymbol{1}$ and $\boldsymbol{\mu} = 1$. The mean square error of the kriging prediction at any untried $\boldsymbol{x}$ is given by

$$MSE\left[\hat{s}_{KR}(\boldsymbol{x})\right] = \hat{\sigma}^2 [1 - \boldsymbol{\rho}(\boldsymbol{x}) \boldsymbol{\Psi}^{-1} \boldsymbol{\rho}^T(\boldsymbol{x}) + \left(1 - \boldsymbol{1}\boldsymbol{\Psi}^{-1}\boldsymbol{\rho}^T(\boldsymbol{x})\right)^2 / \boldsymbol{1}^T \boldsymbol{\Psi} \boldsymbol{1}] \tag{10}$$

In each iteration of the sampling procedure, the global maximum of MSE over the surrogate model domain (10) has to be sought [68]; a new sample is allocated therein [61]. Typically, the global search is realized using population-based metaheuristics, the CPU cost of which is usually high [23], [69]. In this work, an alternative approach is taken, which exploits the particular structure of the surrogate model domain of the nested kriging technique as well as the mathematical formalism defining the domain and its relationships with the normalized domain (a unity interval). More specifically, the maximum of MSE is found in a two-step process, where the first step is exhaustive grid search leading to identification of a good initial point for the subsequent local improvement.

We use the following notation:

- N_0 – initial number of data samples allocated in the surrogate model domain X_S (here, using the method of Section II.B);

- $s_{KR}^{(i)}$ – the second-level surrogate model identified in the i th iteration of the sampling procedure using the current training set $\{\boldsymbol{x}_B^{(k)}, \boldsymbol{R}(\boldsymbol{x}_B^{(k)})\}_{k=1,\ldots,N0+i}$;

Let M_F be a rectangular grid in the objective space F, defined as

$$M_F = \{\boldsymbol{f}^{(k_1,\ldots,k_N)} = [f_1^{k_1}\ f_2^{k_2}\ \ldots\ f_N^{k_N}]^T : : k_j \in \{0, 1, \ldots, N_M\},\ j = 1, \ldots, N\} \quad (11)$$

where $f_j^{k_j} = f_{j.\min} + (k_j/N_M)(f_{j.\max} - f_{j.\min})$. Thus, M_F contains $(N_M + 1)^N$ points uniformly covering F. The initial approximation $\boldsymbol{x}_{\max.tmp}$ of the point maximizing the MSE is found through the exhaustive search on the grid as

$$\boldsymbol{x}_{\max.tmp} = h_2\left([\boldsymbol{f}_{tmp}^T\ 0\ \ldots\ 0]^T\right) \quad (12)$$

where

$$\boldsymbol{f}_{tmp} = \max\{\boldsymbol{f} \in M_F : MSE\ (s_I(\boldsymbol{f}))\} \quad (13)$$

The number of zeros in (12) equals $n - N$. Because the dimensionality of F is low and the first-level model is fast, large values of N_M are utilized in practice (we set $N_M = 100$ in our numerical experiments) without incurring noticeable computational expenditures. This permits relatively precise allocation of the required infill point location.

The design $\boldsymbol{x}_{\max.tmp}$ is refined to obtain the new sample point through local search by solving

$$\boldsymbol{x}_B^{(N_0+i)} = \boldsymbol{x}^* = H(\boldsymbol{z}^*) \quad (14)$$

with

$$\boldsymbol{z}^* = \arg\max_{\boldsymbol{z}\in[0,1]^n}\left\{MSE\left(s_{KR}^{(i)}(H(\boldsymbol{z}))\right)\right\} \quad (15)$$

The starting point for (15) is

$$h_1^{-1}([\boldsymbol{f}_{tmp}^T\ 0\ \ldots\ 0]^T) = H^{-1}(\boldsymbol{x}_{\max.tmp}) \quad (16)$$

The mappings h_1, h_2, and H were defined in Section II.B. The overall design of experiments procedure can be summarized as follows:

1. Allocate the initial sample set $\{\boldsymbol{x}_B^{(k)}\}$ of size N_0 using the method of Section 2.2;
2. Generate a grid M_F (cf. (11)) and set $i = 1$;
3. Set up the second-level kriging surrogate $s_{KR}^{(i)}$ using $\{\boldsymbol{x}_B^{(k)}, \boldsymbol{R}(\boldsymbol{x}^{(k)})\}_{k=1,\ldots,N0+i}$, as the training set;
4. Find the initial approximation $\boldsymbol{x}_{\max.tmp}$ of the MSE maximizer by solving (12), (13);
5. Refine the MSE maximizer (and the new infill sample) $\boldsymbol{x}_B^{(N0+i)}$ by solving (14), (15) with the initial design (16);
6. Set $i = i + 1$;
7. If the termination condition is not satisfied, go to 3;
8. Construct the final second-level surrogate s_{KR} using the current training set.

The termination condition in Step 7 can be based on: (i) exceeding the maximum budget $N_0 + i > N_{\max}$ (user-defined maximum number of samples), (ii) achieving the target value of maximum MSE, or (iii) achieving the target predictive power of the model (estimated using, e.g., cross-validation [70]). Note that (ii) and (iii) do not coincide because the system responses are vector-valued and the error measure applied for model quality assessment may be selected to, e.g., reflect visual agreement between the surrogate-predicted and EM-simulated antenna characteristics. Figure 2 provides a graphical illustration of the overall process of identifying the infill samples.

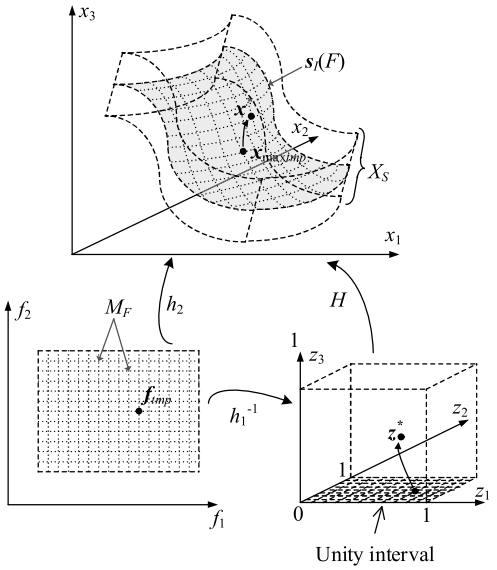

FIGURE 2. Identifying infill samples in sequential design of experiments for the nested-kriging framework. The point ftmp is an initial approximation of the MSE maximizer, found using (13). Its image through the mapping h_2 (cf. (5)) becomes an initial point for local refinement as in (14)-(16); however, optimization process is formally conducted in the unit interval using the mapping H (cf. (6)) mapping the unit interval onto the surrogate model domain X_S.

III. VERIFICATION CASE STUDIES

This section provides numerical verification of the nested kriging with sequential design of experiments, including its comparison with uniform sampling of Section II.B. Our considerations are complemented by discussion that gives a qualitative interpretation of the obtained results.

A. CASE STUDIES

For the sake of numerical verification, the following antenna structures are considered:

- A dual-band uniplanar dipole antenna (Antenna I) shown in Fig. 3(a) [71]. The antenna is implemented on RO4350 substrate ($\varepsilon_r = 3.5$, $h = 0.76$ mm). The EM model is implemented in CST Microwave Studio and evaluated using its time-domain solver (~100,000 cells; simulation time 60 s). The objective is to construct the surrogate model valid for the following ranges of operating frequencies 2.0 GHz $\le f_1 \le$ 3.0 GHz (lower band), and 4.0 GHz $\le f_2 \le$ 5.5 GHz (upper band). The details about the reference designs and the parameter space can be found in [71].
- A trapezoid dual-band dipole antenna (Antenna II) shown in Fig. 3(b) [72]. The structure is implemented

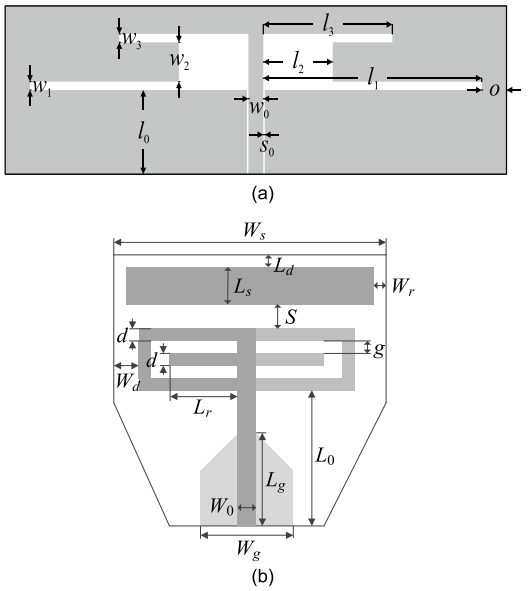

FIGURE 3. Verification case studies: (a) uniplanar dual-band dipole antenna (Antenna I) [71], and (b) trapezoid dual-band dipole antenna (Antenna II) [72].

on RO4003 substrate ($\varepsilon_r = 3.38$, $h = 0.76$ mm) and described by eight independent parameters: $\boldsymbol{x} = [L_{rr}\, dW_s W_d S L_d L_{gr} W_{gr}]^T$ (all dimensions in mm except those with r-subscript which are relative). The parameters $W_r = 5$, $L_s = 5$, and $L_0 = 25$ are fixed. The feed line width $W_0 = 4.5$ mm is calculated to ensure 50 ohm impedance. Other parameters are $L_r = L_{rr}((W_s - W_0)/2 - W_d - d)$, $W_g = W_{gr} W_s$, $L_g = L_{gr}(L_0 - W_g/2 + W_0/2)$, and $g = W_d$. The computational model is implemented in CST Microwave Studio (~900,000 mesh cells, simulation time 250 seconds). In this case, the surrogate model is to be constructed for the objective space parameterized by the operating frequencies f_1 and $f_2 = Kf_1$ for 2.0 GHz $\leq f_1 \leq$ 3.5 GHz, and $1.2 \leq K \leq 1.6$. The details about the reference designs and the parameter space can be found in [72].

B. EXPERIMENTAL SETUP AND RESULTS

For all considered test antennas, the nested kriging surrogate has been constructed using several training sets of various sizes: 100, 200, 400 and 800 samples. In both cases, the surrogate was constructed for two different values of the thickness parameter T (cf. Section II.A). For all cases, the surrogate was constructed using training data allocated according to uniform sampling method of Section II.B as well as sequential DoE of Section II.C. Additionally, a conventional kriging interpolation and radial basis function surrogates have been included to emphasize the overall benefits of the nested kriging framework. The numerical results have been gathered in Tables 1 and 2 for Antennas I and II, respectively.

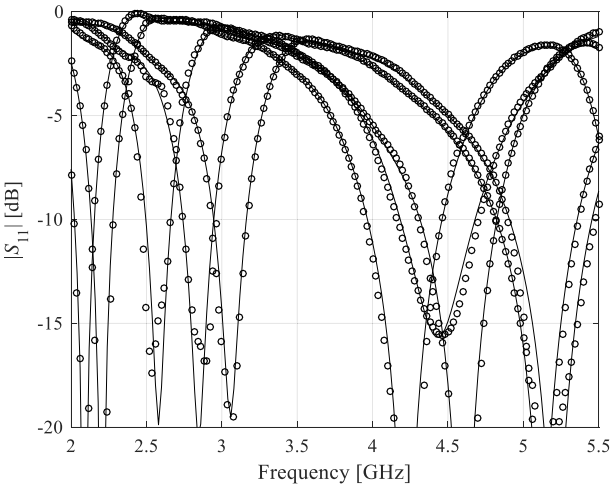

FIGURE 4. Responses of Antenna I at the selected test designs for N = 400: EM model (–), nested kriging surrogate with sequential sampling and D = 0.05 (o).

TABLE 1. Modeling results for Antenna I.

Number of training samples	Relative RMS Error					
	Conventional Models		Nested Kriging with Uniform Sampling (Section II.B)		Nested Kriging with Sequential Sampling (Section II.C)	
	Kriging	RBF	$T = 0.05$	$T = 0.1$	$T = 0.05$	$T = 0.1$
100	17.3 %	19.8 %	4.5 %	6.4 %	4.2 %	6.6 %
200	12.6 %	14.3 %	2.8 %	4.4 %	2.8 %	4.0 %
400	9.3 %	10.5 %	2.6 %	3.8 %	2.2 %	3.6 %
800	7.2 %	8.7 %	2.4 %	3.4 %	1.9 %	3.1 %

TABLE 2. Modeling results for Antenna II.

Number of training samples	Relative RMS Error					
	Conventional Models		Nested Kriging with Uniform Sampling (Section II.B)		Nested Kriging with Sequential Sampling (Section II.C)	
	Kriging	RBF	$T = 0.02$	$T = 0.05$	$T = 0.02$	$T = 0.05$
100	46.7 %	46.9 %	11.2 %	13.5 %	10.8 %	12.2 %
200	41.9 %	44.1 %	6.9 %	7.8 %	6.3 %	8.5 %
400	36.9 %	41.2 %	6.1 %	6.6 %	6.5 %	5.5 %
800	35.5 %	37.5 %	4.1 %	4.9 %	4.5 %	4.8 %

Figures 4 through 5 show the surrogate and EM-simulated antenna responses for the selected test designs.

C. DISCUSSION: WHY SEQUENTIAL SAMPLING DOES NOT IMPROVE MODEL ACCURACY?

The results provided in Tables 1 and 2 clearly demonstrate that sequential DoE does not lead to the improvement of the surrogate model accuracy when compared to uniform sampling of Section II.A. The results are consistent for both considered antennas, various domain thickness parameters T,

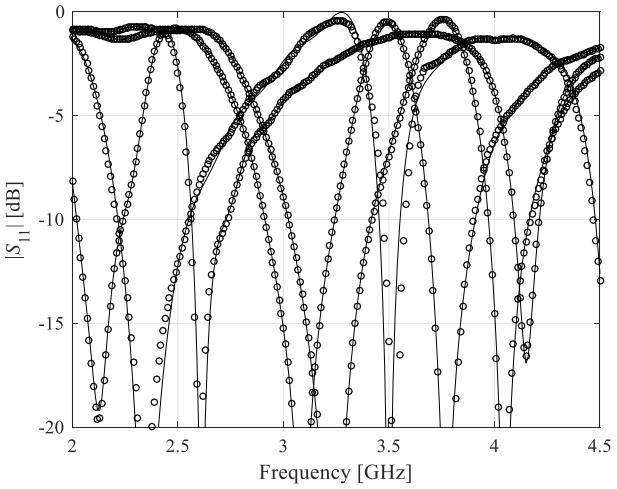

FIGURE 5. Responses of Antenna II at the selected test designs for N = 400: EM model (—), nested kriging surrogate with sequential sampling(o).

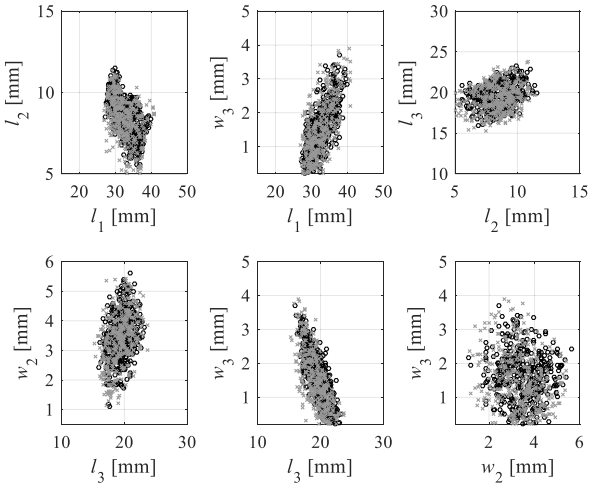

FIGURE 6. Antenna I: selected two-dimensional projections of the training sets obtained using uniform (□) and sequential (o) sampling. It can be observed that the sample distributions for both sets is quite comparable in terms of uniformity, which is an indication that sequential design of experiments does lead to uniform sample allocation when applied to constrained domain of the nested kriging.

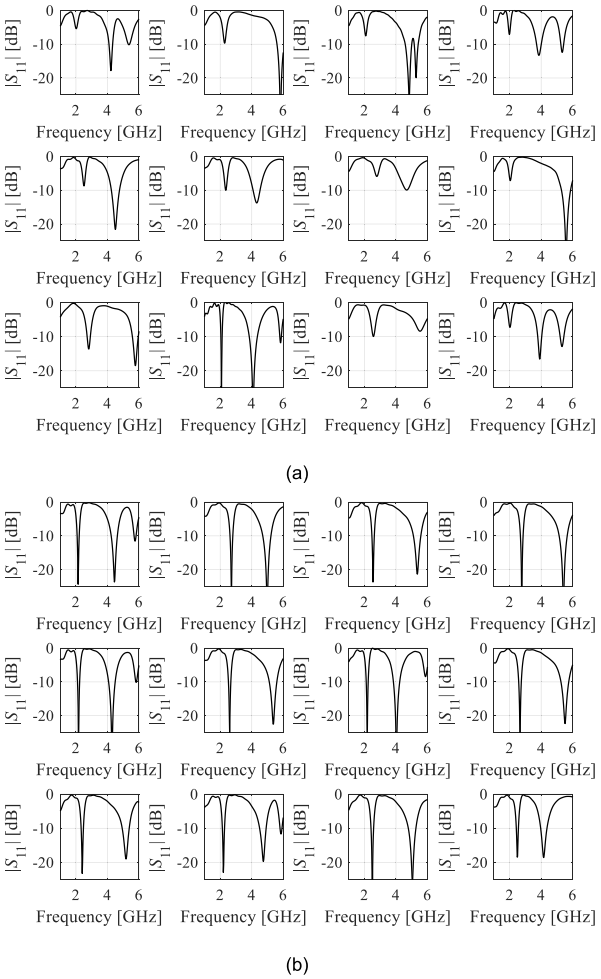

FIGURE 7. Reflection responses of Antenna I at random locations in (a) box-constrained domain X, and (b) constrained domain X_S (cf. Section II.A). Because large regions of the domain X contain poor-quality designs with shallow resonances, the nonlinearity of the functional landscape within X is not uniform and sequential DoE may bring some benefits by concentrating samples in the areas of higher nonlinearities. For the constrained domain, the nonlinearity of the antenna responses is more or less the same throughout X_S (the resonances are deep and just allocated at different frequencies); consequently, uniform sampling seems to be the optimum choice and sequential DoE does not improve the model predictive power.

as well as different training data set sizes. This interesting outcome is counterintuitive and not in line with the intended performance of sequential DoEs.

A closer look into the formulation of the performance-driven surrogates, specifically, nested kriging, helps explaining this phenomenon. The fundamental reason is a very definition of the surrogate model domain, which—by design—contains the parameter vectors that are optimum or nearly-optimum with respect to the performance figures of choice. Because the domain is the extended image of the objective space through the first-level surrogate, it contains uniformly distributed representations of the optimum designs for all combinations of the relevant figures of interest (e.g., operating conditions). This means that the (frequency-averaged) nonlinearity of antenna characteristics is essentially independent of the location within the domain. In particular, there are no regions where the typical nonlinearity of the functional landscape to be modeled is higher than elsewhere.

This is illustrated in Fig. 6 showing random samples distributed within the original (box-constrained) domain X and the constrained domain X_S of the nested kriging. Consequently, uniform distribution of the training samples is what is preferred (from the point of view of improving the global accuracy of the surrogate) and sequential design of experiments leads to such a distribution. Figure 7 provides an illustration for Antenna I, where the distributions obtained using uniform and sequential DoEs are very much comparable.

Based on the above conjectures, the predictive power of the models rendered with uniform and sequential DoEs should indeed be comparable. It appears that (error-wise) optimality of uniform sampling is an inherent feature of performance-driven modeling methods in general, and the nested kriging framework in particular.

IV. CONCLUSION

The paper addressed design of experiments for computationally efficient surrogate modelling of antenna input characteristics. In particular, we compared the performance of the nested kriging modelling framework using uniform (LHS-based) and sequential sampling that involves maximization of the mean square error as the primary infill criterion. Comprehensive numerical experiments conducted for two microstrip antennas lead to counterintuitive results demonstrating no improvement of the predictive power for the surrogate rendered using sequential DoE over the uniform sampling. The results are consistent for all considered test cases, and various sizes of the training sets. This phenomenon has been explained based on the inherent properties of the constrained domain of the nested kriging model, specifically that fact that the domain only contains nearly optimum parameter vectors uniformly representing the design objectives selected for the antenna structure at hand. This leads to a conclusion that uniform sampling seems to be an optimum choice and the improvement due to sequential DoEs (if any) would be negligible. This seems to be an inherent feature of the nested kriging framework as well as other performance-driven modelling techniques.

ACKNOWLEDGMENT

The authors thank Dassault Systemes, France, for making CST Microwave Studio available.

REFERENCES

[1] Q. Li, J. Dong, J. Yang, X. Zhuang, X. Yu, G. Hu, and Y. Guo, "Automated topology optimization of internal antenna design using improved BPSO," in *Proc. Int. Appl. Comput. Electromagn. Soc. Symp. (ACES)*, Suzhou, China, 2017, pp. 1–2.

[2] C. Hu, S. Zeng, Y. Jiang, J. Sun, Y. Sun, and S. Gao, "A robust technique without additional computational cost in evolutionary antenna optimization," *IEEE Trans. Antennas Propag.*, vol. 67, no. 4, pp. 2252–2259, Apr. 2019.

[3] A. Sharma, E. Kampianakis, and M. S. Reynolds, "A dual-band HF and UHF antenna system for implanted neural recording and stimulation devices," *IEEE Antennas Wireless Propag. Lett.*, vol. 16, pp. 493–496, 2017.

[4] J. Dong, W. Qin, and M. Wang, "Fast multi-objective optimization of multi-parameter antenna structures based on improved BPNN surrogate model," *IEEE Access*, vol. 7, pp. 77692–77701, 2019.

[5] X. Zhao, S. P. Yeo, and L. C. Ong, "Planar UWB MIMO antenna with pattern diversity and isolation improvement for mobile platform based on the theory of characteristic modes," *IEEE Trans. Antennas Propag.*, vol. 66, no. 1, pp. 420–425, Jan. 2018.

[6] J. Lundgren, A. Ericsson, and D. Sjoberg, "Design, optimization and verification of a dual band circular polarization selective structure," *IEEE Trans. Antennas Propag.*, vol. 66, no. 11, pp. 6023–6032, Nov. 2018.

[7] J.-F. Qian, F.-C. Chen, K.-R. Xiang, and Q.-X. Chu, "Resonator-loaded multi-band microstrip slot antennas with bidirectional radiation patterns," *IEEE Trans. Antennas Propag.*, vol. 67, no. 10, pp. 6661–6666, Oct. 2019.

[8] Y.-Y. Liu and Z.-H. Tu, "Compact differential band-notched stepped-slot UWB-MIMO antenna with common-mode suppression," *IEEE Antennas Wireless Propag. Lett.*, vol. 16, pp. 593–596, 2017.

[9] K. Saurav, N. K. Mallat, and Y. M. M. Antar, "A three-port polarization and pattern diversity ring antenna," *IEEE Antennas Wireless Propag. Lett.*, vol. 17, no. 7, pp. 1324–1328, Jul. 2018.

[10] R. Leyva-Hernandez, J. A. Tirado-Mendez, H. Jardon-Aguilar, R. Flores-Leal, R. Linares, and Y. Miranda, "Reduced size elliptic UWB antenna with inscribed third iteration sierpinski triangle for on-body applications," *Microw. Opt. Technol. Lett.*, vol. 59, no. 3, pp. 635–641, Mar. 2017.

[11] G.-L. Huang, S.-G. Zhou, and T. Yuan, "Development of a wideband and high-efficiency waveguide-based compact antenna radiator with binder-jetting technique," *IEEE Trans. Compon., Packag., Manuf. Technol.*, vol. 7, no. 2, pp. 254–260, 2nd Quart., 2017.

[12] M. S. Alam and A. M. Abbosh, "Beam-steerable planar antenna using circular disc and four PIN-controlled tapered stubs for WiMAX and WLAN applications," *IEEE Antennas Wireless Propag. Lett.*, vol. 15, pp. 980–983, 2016.

[13] K. D. Xu, D. Li, Y. Liu, and Q. H. Liu, "Printed quasi-yagi antennas using double dipoles and stub-loaded technique for multi-band and broadband applications," *IEEE Access*, vol. 6, pp. 31695–31702, 2018.

[14] T. Cheng, W. Jiang, S. Gong, and Y. Yu, "Broadband SIW cavity-backed modified dumbbell-shaped slot antenna," *IEEE Antennas Wireless Propag. Lett.*, vol. 18, no. 5, pp. 936–940, May 2019.

[15] Y. Liu, S. Wang, X. Wang, and Y. Jia, "A differentially fed dual-polarized slot antenna with high isolation and low profile for base station application," *IEEE Antennas Wireless Propag. Lett.*, vol. 18, no. 2, pp. 303–307, Feb. 2019.

[16] Z. Niu, H. Zhang, Q. Chen, and T. Zhong, "Isolation enhancement for 1×3 closely spaced E-plane patch antenna array using defect ground structure and metal-vias," *IEEE Access*, vol. 7, pp. 119375–119383, 2019.

[17] T. Jhajharia, V. Tiwari, D. Yadav, S. Rawat, and D. Bhatnagar, "Wideband circularly polarised antenna with an asymmetric meandered-shaped monopole and defected ground structure for wireless communication," *IET Microw., Antennas Propag.*, vol. 12, no. 9, pp. 1554–1558, Jul. 2018.

[18] J. Yang, J. Flygare, M. Pantaleev, and B. Billade, "Development of quadruple-ridge flared horn with spline-defined profile for band b of the wide band single pixel feed (WBSPF) advanced instrumentation programme for SKA," in *Proc. IEEE Int. Symp. Antennas Propag. (APSURSI)*, Fajardo, Puerto Rico, Jun. 2016, pp. 1345–1346.

[19] H. J. Gibson, B. Thomas, L. Rolo, M. C. Wiedner, A. E. Maestrini, and P. de Maagt, "A novel spline-profile diagonal horn suitable for integration into THz split-block components," *IEEE Trans. Terahertz Sci. Technol.*, vol. 7, no. 6, pp. 657–663, Nov. 2017.

[20] S. Koziel and S. Ogurtsov, *Simulation-Based Optimization of Antenna Arrays*. Singapore: World Scientific, 2019.

[21] G. Bilgin, V. S. Yilmaz, A. Kara, and E. Aydin, "Comparative assessment of electromagnetic simulation tools for use in microstrip antenna design: Experimental demonstrations," *Microw. Opt. Technol. Lett.*, vol. 61, no. 2, pp. 349–356, Feb. 2019.

[22] S. Koziel and A. Pietrenko-Dabrowska, "Variable-fidelity simulation models and sparse gradient updates for cost-efficient optimization of compact antenna input characteristics," *Sensors*, vol. 19, no. 8, p. 1806, 2019.

[23] M.-C. Tang, X. Chen, M. Li, and R. W. Ziolkowski, "Particle swarm optimized, 3-D-printed, wideband, compact hemispherical antenna," *IEEE Antennas Wireless Propag. Lett.*, vol. 17, no. 11, pp. 2031–2035, Nov. 2018.

[24] S. Koziel and A. Bekasiewicz, "Statistical analysis and robust design of circularly polarized antennas using sequential approximate optimization," in *Proc. 22nd Int. Microw. Radar Conf. (MIKON)*, Poznań, Poland, May 2018, pp. 424–427.

[25] S. Lee, Y. Yang, K.-Y. Lee, K.-Y. Jung, and K. Hwang, "Robust design of 3D-printed 6–18 GHz double-ridged TEM horn antenna," *Appl. Sci.*, vol. 8, no. 9, p. 1582, 2018.

[26] G. Allaire, "A review of adjoint methods for sensitivity analysis, uncertainty quanti-fication, and optimization in numerical codes," Ingenieurs de l'Automobile, SIA, Singapore, Tech. Rep. hal-01242950, Dec. 2015, vol. 836, pp. 33–36.

[27] S. Koziel and A. Bekasiewicz, "Fast EM-driven size reduction of antenna structures by means of adjoint sensitivities and trust regions," *IEEE Antennas Wireless Propag. Lett.*, vol. 14, pp. 1681–1684, 2015.

[28] Y. Zhang, N. K. Nikolova, and M. K. Meshram, "Design optimization of planar structures using self-adjoint sensitivity analysis," *IEEE Trans. Antennas Propag.*, vol. 60, no. 6, pp. 3060–3066, Jun. 2012.

[29] A. Pietrenko-Dabrowska and S. Koziel, "Numerically efficient algorithm for compact microwave device optimization with flexible sensitivity updating scheme," *Int. J. RF Microw. Comput.-Aided Eng.*, vol. 29, no. 7, Jul. 2019, Art. no. e21714.

[30] S. Koziel and A. Pietrenko-Dabrowska, "Reduced-cost electromagnetic-driven optimisation of antenna structures by means of trust-region gradient-search with sparse jacobian updates," *IET Microw., Antennas Propag.*, vol. 13, no. 10, pp. 1646–1652, Aug. 2019.

[31] L. Zappelli, "Optimization procedure of four-port and six-port directional couplers based on polygon equivalent circuit," *IEEE Trans. Microw. Theory Techn.*, vol. 66, no. 10, pp. 4471–4481, Oct. 2018.

[32] S. Koziel and S. Ogurtsov, *Antenna Design by Simulation-Driven Optimization*, Berlin, Germany: Springer, 2014.

[33] J. C. Cervantes-González, J. E. Rayas-Sánchez, C. A. López, J. R. Camacho-Pérez, Z. Brito-Brito, and J. L. Chávez-Hurtado, "Space mapping optimization of handset antennas considering EM effects of mobile phone components and human body," *Int. J. RF Microw. Comput.-Aided Eng.*, vol. 26, no. 2, pp. 121–128, Feb. 2016.

[34] D. Echeverria, D. Lahaye, L. Encica, E. A. Lomonova, P. W. Hemker, and A. J. A. Vandenput, "Manifold-mapping optimization applied to linear actuator design," *IEEE Trans. Magn.*, vol. 42, no. 4, pp. 1183–1186, Apr. 2006.

[35] S. Koziel and S. D. Unnsteinsson, "Expedited design closure of antennas by means of trust-region-based adaptive response scaling," *IEEE Antennas Wireless Propag. Lett.*, vol. 17, no. 6, pp. 1099–1103, Jun. 2018.

[36] L. Leifsson and S. Koziel, "Surrogate modelling and optimization using shape-preserving response prediction: A review," *Eng. Optim.*, vol. 48, no. 3, pp. 476–496, Mar. 2016.

[37] B. Liu, H. Aliakbarian, Z. Ma, G. A. E. Vandenbosch, G. Gielen, and P. Excell, "An efficient method for antenna design optimization based on evolutionary computation and machine learning techniques," *IEEE Trans. Antennas Propag.*, vol. 62, no. 1, pp. 7–18, Jan. 2014.

[38] D. He, C. Liu, T. Q. S. Quek, and H. Wang, "Transmit antenna selection in MIMO wiretap channels: A machine learning approach," *IEEE Wireless Commun. Lett.*, vol. 7, no. 4, pp. 634–637, Aug. 2018.

[39] S. Trehan, K. T. Carlberg, and L. J. Durlofsky, "Error modeling for surrogates of dynamical systems using machine learning," *Int. J. Numer. Methods Eng.*, vol. 112, no. 12, pp. 1801–1827, Dec. 2017.

[40] R. R. Alavi, R. Mirzavand, J. Doucette, and P. Mousavi, "An adaptive data acquisition and clustering technique to enhance the speed of spherical near-field antenna measurements," *IEEE Antennas Wireless Propag. Lett.*, vol. 18, no. 11, pp. 2325–2329, Nov. 2019, doi: 10.1109/LAWP.2019.2938732.

[41] J. E. Rayas-Sanchez and V. Gutierrez-Ayala, "EM-based Monte Carlo analysis and yield prediction of microwave circuits using linear-input neural-output space mapping," *IEEE Trans. Microw. Theory Techn.*, vol. 54, no. 12, pp. 4528–4537, Dec. 2006.

[42] J. Du and C. Roblin, "Stochastic surrogate models of deformable antennas based on vector spherical harmonics and polynomial chaos expansions: Application to textile antennas," *IEEE Trans. Antennas Propag.*, vol. 66, no. 7, pp. 3610–3622, Jul. 2018.

[43] B. Liu, M. O. Akinsolu, N. Ali, and R. Abd-Alhameed, "Efficient global optimisation of microwave antennas based on a parallel surrogate model-assisted evolutionary algorithm," *IET Microw., Antennas Propag.*, vol. 13, no. 2, pp. 149–155, Feb. 2019.

[44] S. Koziel and A. Pietrenko-Dabrowska, *Performance-Driven Surrogate Modeling of High-Frequency Structures*. New York, NY, USA: Springer, 2020.

[45] J. P. C. Kleijnen, "Kriging metamodeling in simulation: A review," *Eur. J. Oper. Res.*, vol. 192, no. 3, pp. 707–716, Feb. 2009.

[46] C. E. Rasmussen and C. K. I. Williams, *Gaussian Processes for Machine Learning*. Cambridge, MA, USA: MIT Press, 2006.

[47] A. I. J. Forrester and A. J. Keane, "Recent advances in surrogate-based optimization," *Prog. Aerosp. Sci.*, vol. 45, nos. 1–3, pp. 50–79, Jan. 2009.

[48] S. Mishra, R. N. Yadav, and R. P. Singh, "Directivity estimations for short dipole antenna arrays using radial basis function neural networks," *IEEE Antennas Wireless Propag. Lett.*, vol. 14, pp. 1219–1222, 2015.

[49] P. Manfredi, D. V. Ginste, I. S. Stievano, D. De Zutter, and F. G. Canavero, "Stochastic transmission line analysis via polynomial chaos methods: An overview," *IEEE Electromagn. Compat. Mag.*, vol. 6, no. 3, pp. 77–84, 2017.

[50] X. Ma and N. Zabaras, "An adaptive high-dimensional stochastic model representation technique for the solution of stochastic partial differential equations," *J. Comput. Phys.*, vol. 229, no. 10, pp. 3884–3915, May 2010.

[51] J. Lee, G.-T. Gil, and Y. H. Lee, "Channel estimation via orthogonal matching pursuit for hybrid MIMO systems in millimeter wave communications," *IEEE Trans. Commun.*, vol. 64, no. 6, pp. 2370–2386, Jun. 2016.

[52] B. Efron, T. Hastie, I. Johnstone, and R. Tibshirani, "Least angle regression," *Ann. Statist.*, vol. 32, no. 2, pp. 407–499, 2004.

[53] D. J. J. Toal and A. J. Keane, "Efficient multipoint aerodynamic design optimization via cokriging," *J. Aircr.*, vol. 48, no. 5, pp. 1685–1695, Sep. 2011.

[54] F. Wang, P. Cachecho, W. Zhang, S. Sun, X. Li, R. Kanj, and C. Gu, "Bayesian model fusion: Large-scale performance modeling of analog and mixed-signal circuits by reusing early-stage data," *IEEE Trans. Comput.-Aided Design Integr. Circuits Syst.*, vol. 35, no. 8, pp. 1255–1268, Aug. 2016.

[55] S. Koziel, "Low-cost data-driven surrogate modeling of antenna structures by constrained sampling," *IEEE Antennas Wireless Propag. Lett.*, vol. 16, pp. 461–464, 2017.

[56] S. Koziel and A. T. Sigurdsson, "Triangulation-based constrained surrogate modeling of antennas," *IEEE Trans. Antennas Propag.*, vol. 66, no. 8, pp. 4170–4179, Aug. 2018.

[57] S. Koziel and A. Bekasiewicz, "On reduced-cost design-oriented constrained surrogate modeling of antenna structures," *IEEE Antennas Wireless Propag. Lett.*, vol. 16, pp. 1618–1621, 2017.

[58] S. Koziel, A. T. Siguresson, and S. Szczepanski, "Uniform sampling in constrained domains for low-cost surrogate modeling of antenna input characteristics," *IEEE Antennas Wireless Propag. Lett.*, vol. 17, no. 1, pp. 164–167, Jan. 2018.

[59] S. Koziel and A. Pietrenko-Dabrowska, "Performance-based nested surrogate modeling of antenna input characteristics," *IEEE Trans. Antennas Propag.*, vol. 67, no. 5, pp. 2904–2912, May 2019.

[60] Z. Liu, M. Yang, and W. Li, "A sequential latin hypercube sampling method for metamodeling," in *Theory, Methodology, Tools and Applications for Modeling and Simulation of Complex Systems*, vol. 643, L. Zhang, X. Song, and Y. Wu, Eds. Singapore: Springer, 2016, pp. 176–185.

[61] J. Liu, Z. Han, and W. Song, "Comparison of infill sampling criteria in kriging-based aerodynamic optimization," in *Proc. 28th Int. Congr. Aeronaut. Sci.*, Brisbane, QLD, Australia, 2012, pp. 23–28.

[62] B. Beachkofski and R. Grandhi, "Improved distributed hypercube sampling," in *Proc. 43rd AIAA/ASME/ASCE/AHS/ASC Struct., Struct. Dyn., Mater. Conf.*, Apr. 2002, p. 1274.

[63] K. Crombecq, E. Laermans, and T. Dhaene, "Efficient space-filling and non-collapsing sequential design strategies for simulation-based modeling," *Eur. J. Oper. Res.*, vol. 214, no. 3, pp. 683–696, Nov. 2011.

[64] J. Kleijnen and W. Beers, "Application-driven sequential designs for simulation experiments: Kriging metamodeling," *J. Oper. Res. Soc.*, vol. 55, no. 8, pp. 876–883, 2004.

[65] J. Kleijnen, "Design and analysis of simulation experiments," in *Statistics and Simulation. IWS 2015. Springer Proceedings in Mathematics & Statistics*, vol. 231, J. Pilz, D. Rasch, V. Melas, and K. Moder, Eds. Cham, Switzerland: Springer, 2018.

[66] S. Koziel, L. Leifsson, I. Couckuyt, and T. Dhaene, "Reliable reduced cost modeling and design optimization of microwave filters using co-kriging," *Int. J. Numer. Model.*, vol. 26, pp. 493–505, Sep. 2013.

[67] M. Kennedy, "Predicting the output from a complex computer code when fast approximations are available," *Biometrika*, vol. 87, no. 1, pp. 1–13, Mar. 2000.

[68] I. Couckuyt, "Forward and inverse surrogate modeling of computationally expensive problems," Ph.D. dissertation, Fac. Eng. Archit., Dept. Inf. Technol., Ghent Univ., Ghent, Belgium, 2013.

[69] A. Bekasiewicz, S. Koziel, and J. W. Bandler, "Low-cost multi-objective design of compact microwave structures using domain patching," in *IEEE MTT-S Int. Microw. Symp. Dig.*, San Francisco, CA, USA, May 2016, pp. 1–3.

[70] S. Arlot and A. Celisse, "A survey of cross-validation procedures for model selection," *Statist. Surv.*, vol. 4, pp. 40–79, 2010.

[71] Y.-C. Chen, S.-Y. Chen, and P. Hsu, "Dual-band slot dipole antenna fed by a coplanar waveguide," in *Proc. IEEE Antennas Propag. Soc. Int. Symp.*, Jul. 2006, pp. 3589–3592, doi: 10.1109/APS.2006.1711396.

[72] M. Qudrat-E-Maula and L. Shafai, "A dual band microstrip dipole antenna," in *Proc. 16th Int. Symp. Antenna Technol. Appl. Electromagn. (ANTEM)*, Victoria, BC, Canada, Jul. 2014, pp. 1–2.

ANNA PIETRENKO-DABROWSKA (Senior Member, IEEE) received the M.Sc. and Ph.D. degrees in electronic engineering from the Gdansk University of Technology, Poland, in 1998 and 2007, respectively. She is currently an Associate Professor with the Gdansk University of Technology. Her research interests include simulation-driven design, design optimization, control theory, modeling of microwave and antenna structures, and numerical analysis.

SLAWOMIR KOZIEL (Senior Member, IEEE) received the M.Sc. and Ph.D. degrees in electronic engineering from the Gdansk University of Technology, Poland, in 1995 and 2000, respectively, the M.Sc. degrees in theoretical physics and in mathematics in 2000 and 2002, respectively, and the Ph.D. degree in mathematics from the University of Gdansk, Poland, in 2003. He is currently a Professor with the School of Science and Engineering, Reykjavik University, Iceland. His research interests include CAD and modeling of microwave and antenna structures, simulation-driven design, surrogate-based optimization, space mapping, circuit theory, analog signal processing, evolutionary computation, and numerical analysis.